Converting NAD-Specific Inositol Dehydrogenase to an Efficient NADP-Selective Catalyst, with a Surprising Twist

ARTICLE *in* BIOCHEMISTRY · AUGUST 2013

Impact Factor: 3.02 · DOI: 10.1021/bi400821s · Source: PubMed

4 AUTHORS, INCLUDING:

Hongyan Zheng
University of Toronto
6 PUBLICATIONS **30** CITATIONS
SEE PROFILE

Drew Bertwistle
Canadian Light Source Inc. (CLS)
10 PUBLICATIONS **118** CITATIONS
SEE PROFILE

David A R Sanders
University of Saskatchewan
59 PUBLICATIONS **940** CITATIONS
SEE PROFILE

BIOCHEMISTRY
including biophysical chemistry & molecular biology

Article

pubs.acs.org/biochemistry

Converting NAD-Specific Inositol Dehydrogenase to an Efficient NADP-Selective Catalyst, with a Surprising Twist

Hongyan Zheng,[†,§] Drew Bertwistle,[†,‡] David A. R. Sanders,[†] and David R. J. Palmer*[,†]

[†]Department of Chemistry, and [‡]Department of Physics and Engineering Physics, University of Saskatchewan, 110 Science Place, Saskatoon, Saskatchewan S7N 5C9, Canada

Supporting Information

ABSTRACT: *myo*-Inositol dehydrogenase (IDH, EC 1.1.1.18) from *Bacillus subtilis* converts *myo*-inositol to *scyllo*-inosose and is strictly dependent on NAD for activity. We sought to alter the coenzyme specificity to generate an NADP-dependent enzyme in order to enhance our understanding of coenzyme selectivity and to create an enzyme capable of recycling NADP in biocatalytic processes. Examination of available structural information related to the GFO/MocA/IDH family of dehydrogenases and precedents for altering coenzyme selectivity allowed us to select residues for substitution, and nine single, double, and triple mutants were constructed. Mutagenesis experiments with *B. subtilis* IDH proved extremely successful; the double mutant D35S/V36R preferred NADP to NAD by a factor of 5. This mutant is an excellent catalyst with a second-order rate constant with respect to NADP of 370 000 s^{-1} M^{-1}, and the triple mutant A12K/D35S/V36R had a value of 570 000 s^{-1} M^{-1}, higher than that of the wild-type IDH with NAD. The high-resolution X-ray crystal structure of the double mutant A12K/D35S was solved in complex with NADP. Surprisingly, the binding of the coenzyme is altered such that although the nicotinamide ring maintains the required position for catalysis, the coenzyme has twisted by nearly 90°, so the adenine moiety no longer binds to a hydrophobic cleft in the Rossmann fold as in the wild-type enzyme. This change in binding conformation has not previously been observed in mutated dehydrogenases.

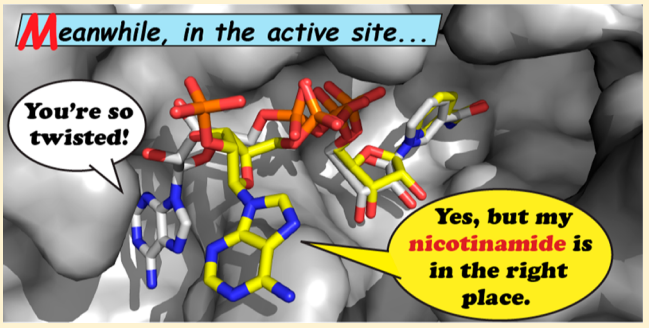

myo-Inositol dehydrogenase (IDH, EC 1.1.1.18) is an enzyme that catalyzes the regiospecific oxidation of the axial hydroxyl

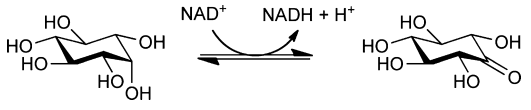

Figure 1. Reaction catalyzed by IDH.

group of *myo*-inositol with concomitant reduction of NAD, as shown in Figure 1.[1,2] Many environmental bacteria, including *Bacillus subtilis*, can utilize *myo*-inositol as the sole carbon source.[3] Inositol catabolism has been linked to important agricultural processes, such as nitrogen fixation in rhizobia, that nodulate pulse crops.[4]

Our laboratory has been studying IDH from *B. subtilis*, and we have revealed that the active site can tolerate a variety of substituted inositol derivatives and related carbohydrates.[5] 1-L-4-O-Substituted derivatives of *myo*-inositol bearing a hydrophobic group, ranging in size from methyl to camphorsulfonyl, are substrates for the enzyme,[6] and some apparently bind more tightly to the enzyme than the natural substrate; 1-L-4-*O*-α-D-glucosyl-*myo*-inositol is oxidized with a virtually identical specificity constant to that for *myo*-inositol.[7] Despite this tolerance for substitution at the 1-L-4-position, the reaction is stereospecific and regiospecific regardless of the substrate. Furthermore, the enzyme shows no detectable activity when NADP replaces NAD in the reaction mixture.

There is considerable interest in the means by which an enzyme can distinguish between NAD and NADP. These coenzymes differ only at the 2′-position of the ribose ring of the adenosine moiety, which is a free hydroxyl group in NAD but bears a phosphate group in NADP. This discrimination in binding is therefore a model case study for molecular recognition determinants. Furthermore, dehydrogenases have found applications in biocatalysis, but the cost-effectiveness of such applications is dependent on the coenzyme. One approach to address this problem is to modify an NADP-dependent enzyme so that it relies on the more stable and less expensive NAD. For example, 2,5-diketo-D-gluconic acid reductase is a valuable catalyst for vitamin C production which strongly prefers NADPH over NADH. Banta et al. engineered the protein to improve NADH-dependent catalysis, resulting in a 7-fold improvement realized mainly through an increase in the turnover number rather than the anticipated improvement in the Michaelis constant.[8] A second approach for making

Received: June 24, 2013
Revised: August 6, 2013

   dx.doi.org/10.1021/bi400821s | *Biochemistry* XXXX, XXX, XXX−XXX

Figure 2. Superposition of the polypeptides of *Z. mobiliz* glucose-fructose oxidoreductase (cyan), *Sinorhizobium morelense* S-30.7.5 1,5-anhydro-D-fructose reductase (magenta), and IDH (yellow). Coordinates from PDB files 2GLX, 1H6D, and 3NT2, respectively.

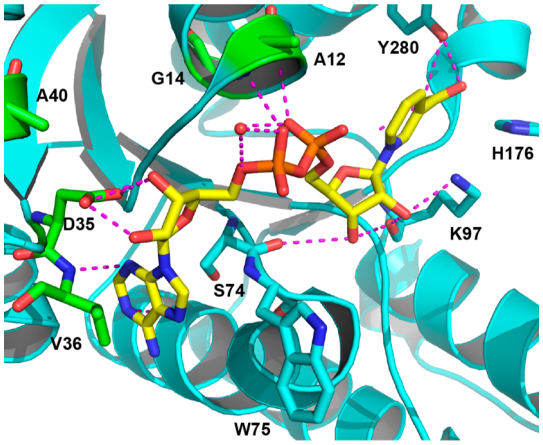

Figure 3. Binding of NAD (yellow) to IDH (cyan). Residues substituted by site-directed mutagenesis in this work, A12, G14, D35, V36, and A40, are shown in green. Also shown is W75 and active site residues S74, K97, Y280, and H176. Polar contacts, as detected by the program PyMol, are shown as magenta dashes.

biocatalysis more cost-effective is through regeneration of the coenzyme. This requires addition of another enzyme (and its substrate), which will convert, for example, NADPH generated in a process back to NADP. By so doing, only a catalytic amount of the coenzyme is required, and the enzyme involved in the process of interest does not need to be altered. Obviously, the recycling enzyme must be convenient and compatible with the system and not reliant on an expensive substrate. Formate dehydrogenase has been used for such purposes, converting formate to CO_2 in an NAD-dependent reaction. That enzyme has been engineered to utilize NADP as well.[9] The endeavor was very successful, taking an enzyme with very low NADP-dependent activity and generating a double mutant with a 10^7-fold higher specificity constant. There are many other examples of switching of coenzyme preference, including phosphite dehydrogenase,[10] glyceraldehyde 3-phosphate dehydrogenase,[11] xylose reductase[12] glucose-fructose oxidoreductase (GFOR),[13] and 1,5-anhydro-D-fructose reductase (AFR).[14] In nearly all cases, the wild-type enzyme is not specific; that is, it can utilize both coenzymes. One exception is engineering of 15-hydroxyprostaglandin dehydrogenase (PGDH), a strictly NAD-dependent enzyme that was converted to an enzyme specific for NADP.[15]

We have previously reported that IDH is stable and 100% active in 20% aqueous DMSO and retains most of its activity in up to 40% DMSO and in up to 15% aqueous methanol. We have also observed that IDH is active after adsorption onto Celite, suggesting this enzyme is a good candidate for engineering toward catalytic applications. Because *myo*-inositol is cheap, nontoxic, water-soluble, and neutral, IDH would make a good coupling enzyme for recycling of coenzyme. This led us to engineer an NADP-dependent catalytic ability into this NAD-specific enzyme.

The existing examples in the literature gave us a guide for engineering the enzyme. Furthermore, we have previously reported the high-resolution structure of IDH in complex with NAD, so we have a structural basis for design.[16] IDH is a member of the GFOR/IDH/MocA family of enzymes. Proteins in this family are made up of an *N*-terminal Rossmann fold and *C*-terminal α/β domain notable for the extensive (usually eight-stranded) β-sheet structure in each monomer. The active site is found in a cleft at the interface of the two domains. IDH is active as a tetramer, with each monomer contributing to a central series of β-strands that hold the tetramer together. The four active sites are independent, however, showing no cooperativity in catalysis.

Other structurally and functionally characterized members of this family of enzymes include *Zymomonas mobilis* GFOR and *Sinorhizobium morelense* S-30.7.5 AFR. Both of these enzymes are NADP-dependent. In the case of GFOR, the coenzyme is tightly bound and is not released during its catalytic cycle. Both of these enzymes have been engineered to accept NAD as a coenzyme, which was particularly useful for our design. Although the Rossmann fold domains of dehydrogenases all complex NAD(P) in approximately the same way, there is considerable variation in the residues involved, and the domain itself may be found in a variety of protein contexts; that is, they may be N-terminal, C-terminal, or central domains and may be found in different orientations relative to the rest of the protein. Formate dehydrogenase, for example, contains a Rossmann fold from residues 128 to 311 of the 364 amino acid protein, and the overall protein fold bears no resemblance to that of IDH.

GFOR and AFR have the same overall fold as IDH, as shown in Figure 2. There are some notable differences, however, in the coenzyme binding. GFOR, which does not release its coenzyme during reaction, makes 32 polar contacts with NADP. Perhaps predictably, fewer such contacts are observed between AFR and its reversibly bound coenzyme, and the same is true for IDH (Figure 3, and Figure S1 in Supporting Information).

Naturally, the key changes in the protein predicted to alter coenzyme recognition are those near the 2′-position of the adenine moiety. In most NAD-dependent enzymes, an aspartate residue can be identified that forms hydrogen bonds with the ribose. The negatively charged carboxylate would effectively repel a phosphate group in this position. A consensus motif $GXGXXGX_{17-18}D$ can be used to pinpoint the aspartate (or sometimes glutamate) residue. NADP-dependent enzymes typically replace the aspartate or glutamate with a small, neutral residue, commonly serine. It is also common to find a positively charged residue near this position, in or near the loop between $\beta 2$ and $\alpha 2$ of the Rossmann fold domain, that may either interact with the 2′-phosphate group or form a cation$-\pi$

dx.doi.org/10.1021/bi400821s | *Biochemistry* XXXX, XXX, XXX−XXX

stacking interaction with the adenine moiety,[17] but the presence of such a residue is not necessary.[18] It has also been postulated that the overall electrostatic nature of the pocket is an important discriminating factor.[11]

Beyond these differences that can be rationalized on the basis of charge difference, there are apparently empirical differences that have also been observed. For example, the third glycine residue of the consensus motif (GXGXXG) is often replaced by an alanine in NADP-dependent dehydrogenases, including GFOR. Similarly, a lysine residue is often found in NADP-dependent enzymes at the beginning of α1 of the Rossmann fold, which is near the diphosphate group of the coenzyme. Because both NAD and NADP contain this diphosphate, the reason for this preference is not obvious.

On the basis of the experiments on the homologous enzymes GFOR and AFR, and the very successful alteration of the short chain dehydrogenase PGDH, we selected a series of residues to test the apparent rules for coenzyme switching with the intent of generating an efficient NADP-dependent IDH mutant and solving the high-resolution structure of such a mutant bound to NADP.

MATERIALS AND METHODS

All reagents, including buffers, salts, *myo*-inositol, NAD, and NADP, were obtained from Sigma-Aldrich Canada, Ltd. (Oakville, Ontario, Canada) or VWR CanLab (Mississauga, Ontario, Canada) and were categorized as molecular biology grade or were of the highest grade available. IDH and its mutants were generated and expressed, and the resulting proteins were purified and assayed as described previously.[6] Site-directed mutants were generated using the QuikChange Site-Directed Mutagenesis Kit from Stratagene, following the manufacturer's instructions. All resulting mutants were sequenced by the DNA Technologies Unit of the National Research Council, Saskatoon, Canada. A table of mutagenic primer sequences is provided in the Supporting Information.

Kinetic constants were determined using the program Leonora,[19] which was also used to evaluate cooperativity. Data were fit to the equation for a compulsory, ordered bi-bi mechanism (eq 1):

$$v = \frac{V_{max}[A]^h[B]}{K_{iA}K_{mB} + K_{mB}[A]^h + K_{mA}^h[B] + [A]^h[B]} \quad (1)$$

where A is NAD(P), B is inositol, K_{mA} and K_{mB} are the respective Michaelis constants, K_{iA} is the inhibitory binding constant of NAD(P), and h is the Hill coefficient. In nearly every case, h = 1. Exceptions were mutants G35S in the presence of NADP, G14A/D35S in the presence of NAD, and G14A/D35S in the presence of NADP. All kinetic assays were performed in triplicate at 25 °C in 100 mM Tris−HCl, pH 9.0. Reactions were monitored at 340 nm to detect the appearance of NADH or NADPH (ε_{340} = 6220 M^{-1} cm^{-1}).

Crystallization. Expression and purification of protein for crystallization was described previously.[20] Purified protein stock was thawed and diluted 1:1 with 25 mM Tris−HCl, pH 8.0, to a concentration of 3.25 mg mL^{-1} and incubated with 10 mM of NADPH, on ice, for 30 min. Crystal screening was done using the microbatch technique against crystallization screens from Qiagen. Crystallization drops were made by adding 1 μL of crystallization buffer to 1 μL of protein, and a layer of paraffin oil was overlaid to slow evaporation. Plates were stored at room temperature and single crystals grew within a few days. Two conditions yielded crystals with >100 μm edge length and with well-defined morphology: Classic II, #29 (0.96 M sodium citrate, pH 7.0); Classic II, #92 (0.1 M magnesium formate, 15% (w/v) PEG 3350). In the subsequent structure analysis, we found clear density for the cofactor in the latter (binary structure) and an absence of density for the cofactor in the former (apo). The crystals were cryo-protected by a mixture of 37.5% ethylene glycol, 37.5% crystallization solution, and 12.5% 25 mM Tris−HCl, pH 8.0, and flash cooled in liquid nitrogen.

Table 1. Data Collection and Scaling Statistics

enzyme	IDH A12K/D35S:apo	IDH A12K/D35S:NADP
wavelength (Å)	0.9791	0.9794
space group	*I*222	$P2_1$
unit cell lengths (Å)	a = 52.07, b = 121.11, c = 128.47	a = 50.63, b = 190.29, c = 90.24
unit cell angles (deg)	α = 90.00, β = 90.00, γ = 90.00	α = 90.00 β = 100.31 γ = 90.00
resolution (Å)	48.26−6.17 (2.06−1.95)	51.61−6.61 (2.20−2.09)
observed reflections	13 160 (64 305)	22 367 (99 413)
unique reflections	1 020 (4 326)	3 047 (14 322)
completeness (%)	97.7 (100)	95.2 (98.9)
multiplicitly	12.9 (14.9)	7.3 (6.9)
mean ($I/\sigma(I)$)	30.5 (5.1)	34.6 (4.9)
R_{merge} [b]	0.06 (0.56)	0.04 (0.33)
average mosaicity	0.39	0.42
detector distance (mm)	250	280
oscillation angle (deg)	1.0	0.5
exposure time (s)	0.5	0.5
Refinement Statistics		
cofactor molecules		NDP
R_{work}/R_{free} [c]	19/23	19/23
Ramachandran Plot (%)		
favored	97.9	97.6
outliers	0	0.3
RMS Deviations from Ideal Values		
bonds (Å)	0.007	0.008
angles (deg)	1.02	1.11
Average *B* Factors (Å^2)		
overall	32.77	45.06
protein + cofactor	32.77	45.20
water molecules	32.82	38.17

[a]Data collection and scaling statistics were calculated in MOSFLM and SCALA, respectively. [b]The merging R factor was calculated using $R_{merge} = \Sigma_h\Sigma_i|I_{hl} - \langle I_h\rangle|/\Sigma_h\Sigma_l\langle I_h\rangle$. [c]$R$ factors were calculated using $R = \Sigma(||F_{obs}| - |F_{calc}||)/\Sigma|F_{obs}|$, where F_{obs} and F_{calc} are the observed and calculated structure factors and R_{free} was calculated using 5% of the data collected. Average B factors were calculated using PHENIX.

X-ray Data Collection and Processing. Diffraction data was collected at the CLS protein crystallography undulator beamline, ID08. Although the data collection conditions varied slightly, their data processing treatment was similar. The flash-cooled cryo-protected crystals were mounted under a dry nitrogen cryo stream, and diffraction images were measured over a 180° rotation. Images were integrated in the program MOSFLM[21] and then subsequently merged and scaled using

dx.doi.org/10.1021/bi400821s | *Biochemistry* XXXX, XXX, XXX−XXX

Table 2. Steady-State Kinetic Constants for Wild-Type and Mutated IDH

enzyme	coenzyme	$K_m^{NAD(P)}$ (mM)	$K_m^{inositol}$ (mM)	k_{cat} (s^{-1})	$k_{cat}/K_m^{NAD(P)}$ (s^{-1} M^{-1})	$(k_{cat}/K_m^{NADP})/(k_{cat}/K_m^{NAD})$
wild-type IDH	NAD	0.08 ± 0.01	4.4 ± 0.5	42 ± 2	5.3×10^5	$<10^{-5}$ [a]
G14A	NAD	0.15 ± 0.02	4.7 ± 0.9	30 ± 1	2.0×10^5	$<10^{-5}$
	NADP	trace activity	trace activity	trace activity	trace activity	
D35S	NAD	1.7 ± 0.1	22 ± 7	150 ± 4	8.9×10^4	0.6
	NADP	2.3 ± 1.0	809 ± 261	114 ± 29	5.0×10^4	
G14A/D35S	NAD	3.4 ± 2.9	259 ± 71	32 ± 4	1.0×10^4	0.1
	NADP	30 ± 16	190 ± 90	26 ± 11	9.0×10^2	
A12K/D35S	NAD	1.9 ± 0.3	16 ± 7	176 ± 7	9.5×10^4	1.0
	NADP	1.7 ± 0.8	185 ± 91	153 ± 21	9.3×10^4	
D35S/V36R	NAD	1.8 ± 0.2	7.4 ± 5.6	118 ± 10	6.5×10^4	5.7
	NADP	0.16 ± 0.02	35 ± 4	59 ± 2	3.7×10^5	
A12K/D35S/V36R	NAD	1.2 ± 0.2	4.2 ± 0.6	139 ± 7	1.2×10^5	4.9
	NADP	0.06 ± 0.01	24 ± 2	34 ± 2	5.7×10^5	
D35S/A40K	NAD	2.8 ± 0.8	9.0 ± 2.0	184 ± 11	6.6×10^4	2.3
	NADP	0.9 ± 0.2	41 ± 18	146 ± 8	1.6×10^5	
D35S/V36R/A40K	NAD	0.9 ± 0.1	25 ± 5	84 ± 6	9.3×10^4	3.8
	NADP	0.04 ± 0.01	8.5 ± 1.3	14 ± 1	3.5×10^5	

[a]No apparent activity was detected for the wild-type IDH with NADP. The estimated upper limit is based on the spectrophotometer detection limit at [IDH] = 100 nM, [NAD] = 10 mM.

the program SCALA.[22] Prior to merging, POINTLESS[22] was used to determine the crystal space group for the apo and binary structures as $I222$ and $P2_1$, respectively.

The apo and binary crystal structures were solved by the molecular replacement method[23] using the program MOLREP[24,25] with the wild-type IDH structure as the search template, RSCB Protein Data Bank (PDB) accession 3MZ0.[16] The apoenzyme crystal yielded one monomer in the asymmetric unit, whereas the binary complex structure gave four monomers; the Matthews coefficients[26] were 2.70 and 2.85, respectively.

Refinement of the structures and modeling into electron density maps was completed by alternating between the programs PHENIX[27] and COOT.[28] Initial refinement steps included three macrocycles of simulated annealing to mitigate model bias and a round of rigid body refinement. All subsequent refinement steps included three macrocycles of individual coordinate refinement, individual isotropic B-factors, and occupancies of select atoms. NCS restraints were applied throughout all refinements with the exception of the last refinement step.

Inspection of the binary structure $F_o - F_c$ map identified electron density for the cofactor at the location of the Rossmann fold α helix. A NADPH coordinate model was obtained from the Heterocompound Information Centre,[24] energy minimized in eLBOW,[29] and manually modeled into the $F_o - F_c$ density. Ramachandran statistics of both structures were calculated using the program MOLPROBITY.[30] Data processing results and statistics are summarized in Table 1. The crystal structure data of the double mutant A12K/D35S are deposited are deposited in the PDB as 4L9R (apoenzyme) and 4L8V (NADP complex).

RESULTS AND DISCUSSION

Site-Directed Mutagenesis. The key residue in IDH for discrimination between NAD and NADP is the aspartate residue Asp35 (Figure 3). This residue, located on a loop between $\beta 2$ and $\alpha 2$ of the Rossmann fold, forms hydrogen bonds with the 2′- and 3′-hydroxyl groups of the adenosyl moiety of the coenzyme. As mentioned above, the negatively charged residue in this position is typically replaced with a small, neutral amino acid, frequently serine, in NADP-binding proteins. Substitution of Asp35 with serine in IDH results in a mutant able to utilize both NAD and NADP as coenzymes in the dehydrogenation of inositol. This is in accord with the inverse experiment reported by Baker with GFOR.[13] In that case, the S116D mutant was a dual-specificity enzyme, but it still preferred the native coenzyme, NADP, for the dehydrogenation of glucose. However, GFOR S116D was not an efficient catalyst ($k_{cat}/K_m < 10^2$ M^{-1} s^{-1}). The IDH mutant D35S also retained preference for the native coenzyme, NAD, although only slightly (as shown in Table 2). Encouragingly, the resulting second-order rate constant for reaction of NADP was comparable to that of wild-type IDH with NAD. However, the Michaelis constant for *myo*-inositol using NADP as a cofactor increased by about 2 orders of magnitude as a result of this mutation.

Alteration of the adjacent residue, Val36, to arginine was intended to introduce a positive charge in the putative 2′-phosphate-binding region of the enzyme. A positive charge is not consistently found in this region in NADP-dependent enzymes, but precedent suggested that this strategy would be effective.[12,15] The resulting double mutant, D35S/V36R, was a strikingly good catalyst for dehydrogenation of inositol, with a second-order rate constant improved 10-fold compared to that of the single mutant D35S and a greatly reduced inositol Michaelis constant. Moreover, this enzyme now shows a greater than 5-fold preference for NADP over NAD.

Gly14, the third glycine residue of the consensus motif (GXGXXG), is replaced by an alanine residue in the analogous position of GFOR. In studying NADP-dependent AFR, Dambe et al. found that the analogous Ala13 "is crucial for the discrimination between NADPH and NADH".[14] We therefore generated G14A to test the generality of the role of the residue in this position. As shown in Table 2, this mutation had a very small effect on the enzyme. The double mutant G14A/D34S was not an improvement over D35S, showing a greater selectivity for NAD. A comparison of the structures of IDH with AFR and GFOR shows that the fold differs slightly in this

dx.doi.org/10.1021/bi400821s | Biochemistry XXXX, XXX, XXX–XXX

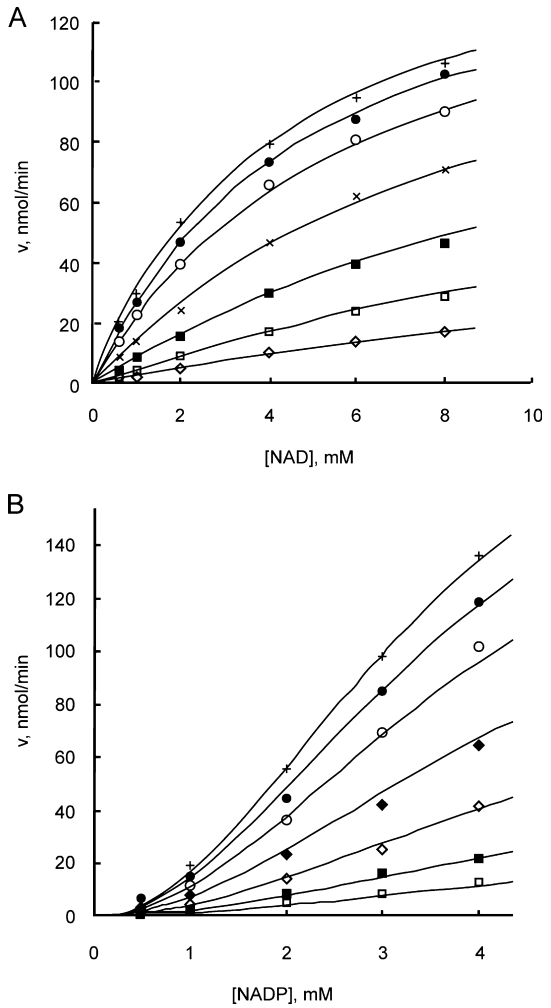

Figure 4. Effect of coenzyme on the rate of D35S-catalyzed oxidation of inositol. (A) Dependence on [NAD], h = 1. [Inositol] = 20 mM (◇), 40 mM (□), 80 mM (■), 160 mM (×), 320 mM (○), 500 mM (●), 700 mM (+). (B) Dependence on [NADP], h = 2. [Inositol] = 20 mM (□), 40 mM (■), 80 mM (◇), 160 mM (◆), 320 mM (○), 500 mM (●), 700 mM (+).

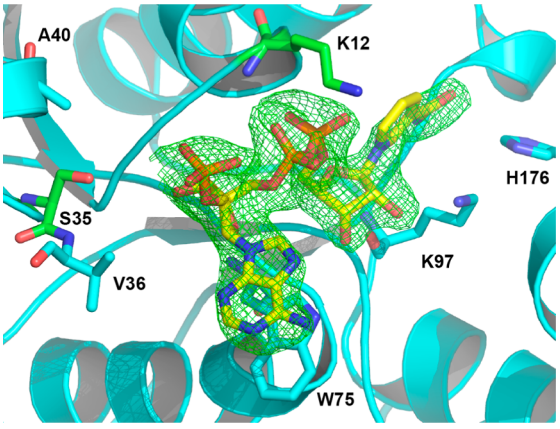

Figure 5. Binding of NADP to A12K/D35S. Residues in green are the results of mutation. The $2F_o - F_c$ density of the coenzyme, contoured to 1σ, is shown in green mesh.

region so that the consensus sequence does not sit in precisely the same place in the Rossmann fold.

Examination of the high-resolution crystal structure of IDH shows that Ala12 sits in a short loop between β1 and α1 of the Rossmann fold, essentially at the base of the first helix (Figure 3). This residue is structurally analogous to Gln15 of 15-PGDH. This residue was substituted with lysine in order to convert that enzyme from NAD to NADP dependence.[15] We therefore introduced a lysine residue at this position in the D35S and D35S/V36R mutants. The double mutant A12K/D35S showed very similar catalytic constants to the D35S mutant with respect to NAD but improved catalysis and apparent recognition of inositol in the presence of NADP, such that the double mutant showed identical second-order rate constants with respect to coenzyme. The triple mutant, A12K/D35S/V36R, showed a nearly 5-fold preference for NADP and a notably smaller Michaelis constant for NADP than D35S and A12K/D35S. The second-order rate constant with respect to NADP for this mutant exceeds that of the wild-type IDH with NAD.

The crystal structure of IDH bound to NAD indicated that Ala40, found on α2 near the 2′-hydroxyl of the bound adenine moiety (Figure 3), was a good candidate for mutagenesis. Introduction of a positively charged residue in this position was predicted to provide a potentially stabilizing environment for the binding of the 2′-phosphate group of NADP. Therefore, double mutant D35S/A40K and triple mutant D35S/V36R/A40K were generated and examined.

The introduction of the lysine residue in position 40 of the D35S mutant had only a very small effect on the NAD-dependent reaction but as predicted improved every kinetic constant for the NADP-dependent reaction, resulting in a switch in NADP/NAD preference from 0.6 to 2.3. The triple mutant D35S/V36R/A40K, when compared with D35S/V36R, showed similar catalytic constants with respect to NAD, but the Michaelis constant for inositol increased 3-fold. In the presence of NADP, the Michaelis constants for both substrate and coenzyme improved over D35S/V36R, but k_{cat} decreased 4-fold. The coenzyme selectivity strongly favored NADP but not as much as for the double mutant.

Unexpectedly, some mutations resulted in cooperativity with respect to coenzyme. Specifically, the D35S-catalyzed reaction showed cooperativity with respect to NADP but not NAD. A Hill coefficient of 2.0 was required to fit the data for the dependence of rate on NADP as shown in Figure 4. The double mutant G14A/D35S showed similar cooperativity with respect to NAD and NADP. No other mutants showed cooperativity in catalysis, and such behavior has not been reported in similar studies of which we are aware. Notably, the dependence of rate on inositol showed no cooperativity for any of the mutants. IDH follows a compulsory ordered bi-bi mechanism in which the coenzyme binds first, followed by inositol. These results suggest that for these select mutants, the apoenzyme is altered such that the coenzyme binding affects the tetrameric structure and promotes further binding of coenzyme. The coenzyme-bound form of each mutant behaves as observed for wild-type IDH, with each active site acting independently.

Crystallography. The A12K/D35S mutant was successfully crystallized as the apoenzyme and in complex with NADP to 1.95 and 2.09 Å resolution, respectively. Structural alignment of the mutant and wild-type structures (PDB: 3MZ0) revealed close conservation of structure as indicated by the α-carbon root mean squared deviation (rmsd) of 0.29 Å (Figure S2, Supporting Information). Similarly, the NADP-bound structure of the double mutant showed little deviation from the wild-type

dx.doi.org/10.1021/bi400821s | *Biochemistry* XXXX, XXX, XXX–XXX

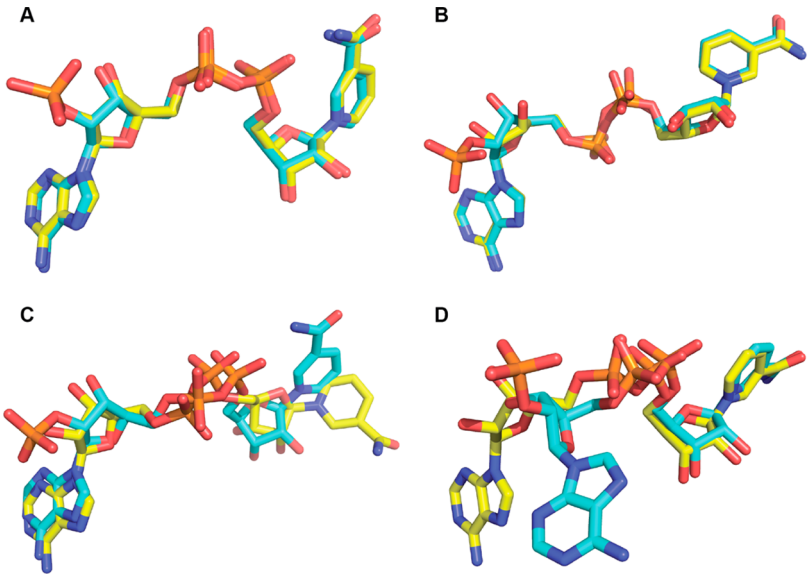

Figure 6. Binding conformation of NAD (yellow) and NADP (cyan) in the crystal structure of (A) glyceraldehyde-6-phosphate dehydrogenase triple mutant (data from 1DBV, 2DBV), (B) xylose reductase mutant (1YE4, 1YE6), (C) glucose-6-phosphate dehydrogenase mutants (1H9A, 1H94), and (D) wild-type IDH and A12K/D35S.

NAD-bound structure (rmsd = 0.32 Å). Structural alignment of the A12K/D35S apo- and NADP-bound structures results in an rmsd = 0.55 Å, which was similar to the deviation shown between wild-type IDH apo- and holo-enzyme α-carbon backbones (0.58 Å). The greater deviation in the backbone upon coenzyme complexation suggests a small but significant conformational effect, which is consistent with the compulsory ordered mechanism of the IDH-catalyzed reaction.

Chain A of the apo- and NADP-bound structures of A12K/D35S were analyzed for dynamic domain movement using the DynDom database of protein domain motions.[31,32] This analysis found that NADP binding induces a main bend at residues 123−124, the natural separation between the N-terminal Rossmann fold domain (1−123) and the C-terminal domain (124−324).[16] The C-terminal domains of the structures are superimposed with an rmsd of 0.27 Å, and the N-terminal domain rotates by 5.3° about a hinge axis (Figure S3, Supporting Information). Effectively, binding of NADP results in N-terminal domain movement toward the C-terminal domain by ∼1 Å, tightening the binding pocket.

The electron density for the coenzyme in chain A was apparent at 3σ in the $F_o - F_c$ with a post refinement occupancy of 0.87. The bound coenzyme is shown in Figure 5 (also Figure S4, Supporting Information). The other three cofactor binding sites were less well-defined though still clear at 3σ for the diphosphate. Occupancy refinement in these three sites resulted in partial occupancies of 0.63, 0.65, and 0.60 for chains B, C, and D, respectively. Notable is the conformation of K97, an active-site residue required for activity. Previous IDH crystal structures showed that when NAD is bound to the active site, the ε-nitrogen of K97 forms a hydrogen bond with the coenzyme, specifically with the 2′-hydroxyl group of the nicotinamide ribose. When NADH is bound, this residue shifts, making a hydrogen bond with H176. These two residues are likely part of a proton relay that accepts the proton of the hydroxyl group undergoing oxidation in the reaction.[16] The crystal structure of the A12K/D35S mutant shows K97 hydrogen-bonded to the 2′-hydroxyl of the coenzyme, indicating that it is the oxidized form of the coenzyme that is observed bound to the protein.

The 2′-phosphate of NADP was expected to sit in an empty pocket created by the D35S mutation. Instead, the phosphate is rotated away from the pocket, and the adenine ring forms an apparent π-stacking interaction with W75. The structure of the wild-type enzyme in complex with NAD, PDB 3NT2,[16] was used to compare the relative positions of NAD and NADP in the wild-type and mutant crystal structures, respectively. A least-squares superposition was performed using residues 190−250 of the mutant structure as a target, resulting in an rmsd deviation of 0.2 Å. The pyrophosphate region of the coenzyme in the two structures remains relatively fixed at the end of helix α1, typical of binding to the Rossmann fold. However, the 2′-phosphate of the coenzyme sits such that the entire ribose ring has turned, twisting the adenosyl moiety and allowing the aromatic base to π-stack with the indole of W75. The resulting structure maintains the nicotinamide ring in an essentially identical position to that in the wild-type structure, whereas the position of the amino group of the adenine has changed by nearly 11 Å.

Dehydrogenases mutated to become nonselective with respect to coenzyme have been crystallized previously in the presence of the newly accepted coenzyme. Examples include the NAD-specific *Bacillus stearothermophilus* glyceraldehyde-3-phosphate dehydrogenase, which was altered to a triple mutant that favors NADP, although the mutant is a poorer catalyst than the wild-type enzyme. The mutant was crystallized in complex with NAD (1DBV) and NADP (2DBV), and the coenzyme binds in a nearly identical orientation in each case, as shown in Figure 6A. Similarly, the *Candida tenuis* xylose reductase K274R mutant, which shows almost no discrimination between NAD and NADP, also binds both coenzymes in a very similar orientation (Figure 6B).[33] The *Leuconostoc mesteroides* glucose-6-phosphate dehydrogenase is a dual-specificity enzyme that has been crystallized with both coenzymes.[34] Although the nicotinamide portion of NAD appears to be in a different orientation from that of NADP (Figure 6C), the authors point out that this region of the cofactor is of low occupancy and

dx.doi.org/10.1021/bi400821s | *Biochemistry* XXXX, XXX, XXX−XXX

should be considered disordered. The adenosine/adenosine-2′-phosphate moieties of the two coenzymes, however, again show a very similar orientation. Thus, the twist in NADP binding to IDH A12K/D35S stands out from these structures.

In conclusion, we have generated an efficient catalyst for NADP-dependent dehydrogenation of *myo*-inositol, requiring only two mutations to generate activity that was completely absent in the wild-type enzyme. This demonstrates the evolutionary flexibility incorporated into the Rossmann fold for nucleotide binding, such that under selective pressure, a new catalyst could be generated easily by an organism. This rational approach achieved equally good or better results than directed evolution experiments for altering coenzyme selectivity.[9,35]

■ ASSOCIATED CONTENT

Supporting Information

Table of mutagenesis primers, figures depicting cofactor binding generated using Ligplot, tetramer structure of wild-type and A12K/D35S IDH, and domain movement calculated by DynDom. This material is available free of charge via the Internet at http://pubs.acs.org.

■ AUTHOR INFORMATION

Corresponding Author

*D.R.J.P. E-mail: dave.palmer@usask.ca. Phone: (306) 966-4662. Fax: (306) 966-4730.

Present Address

§H.Z., Department of Chemical Engineering and Applied Chemistry, University of Toronto.

Funding

This work was funded by a Natural Sciences and Engineering Research Council of Canada (NSERC) Discovery Grants to D.A.R.S and D.R.J.P. and by the Saskatchewan Health Research Foundation (S.H.R.F.) through support for the Molecular Design Research Group.

Notes

The authors declare no competing financial interest.

■ ACKNOWLEDGMENTS

The authors thank Ken Thoms, Dr. Keith Brown, the other staff of the Saskatchewan Structural Sciences Centre, and Dr. Karin van Straaten for helpful discussions. We thank the staff of macromolecular beamline 08ID-1, Canadian Light Source (CLS), Saskatoon, Saskatchewan, Canada, for their technical assistance during data collection. The structural studies described in this paper were performed at the CLS, which is supported by NSERC, the National Research Council of Canada, the Canadian Institutes of Health Research, the Province of Saskatchewan, Western Economic Diversification Canada, and the University of Saskatchewan.Abbreviations

AFR, 1,5-anhydro-D-fructose reductase; GFOR, glucose-fructose oxidoreductase; IDH, *Bacillus subtilis myo*-inositol 2-dehydrogenase; NAD, nicotinamide adenine dinucleotide (oxidized form); NADH, nicotinamide adenine dinucleotide (reduced form); NADP, nicotinamide adenine 2′-phosphate dinucleotide (oxidized form); NADPH, nicotinamide adenine 2′-phosphate dinucleotide (reduced form); PDB, Protein Data Bank; RCSB, Research Collaboratory for Structural Bioinformatics

■ REFERENCES

(1) Ramaley, R., Fujita, Y., and Freese, E. (1979) Purification and properties of Bacillus subtilis inositol dehydrogenase. *J. Biol. Chem. 254*, 7684−7690.

(2) Daniellou, R., Zheng, H., and Palmer, D. R. J. (2006) Kinetics of the reaction catalyzed by inositol dehydrogenase from Bacillus subtilis and inhibition by fluorinated substrate analogs. *Can. J. Chem. 84*, 522−527.

(3) Yoshida, K. I., Aoyama, D., Ishio, I., Shibayama, T., and Fujita, Y. (1997) Organization and transcription of the myo-inositol operon, iol, of Bacillus subtilis. *J. Bacteriol. 179*, 4591−4598.

(4) Kohler, P. R. A., Zheng, J. Y., Schoffers, E., and Rossbach, S. (2010) Inositol Catabolism, a Key Pathway in Sinorhizobium meliloti for Competitive Host Nodulation. *Appl. Environ. Microbiol. 76*, 7972−7980.

(5) Daniellou, R., Phenix, C. P., Tam, P. H., Laliberte, M. C., and Palmer, D. R. J. (2005) Stereoselective oxidation of protected inositol derivatives catalyzed by inositol dehydrogenase from Bacillus subtilis. *Org. Biomol. Chem. 3*, 401−403.

(6) Daniellou, R., Zheng, H., Langill, D. M., Sanders, D. A. R., and Palmer, D. R. J. (2007) Probing the promiscuous active site of myo-inositol dehydrogenase using synthetic substrates, homology modeling, and active site modification. *Biochemistry 46*, 7469−7477.

(7) Daniellou, R., and Palmer, D. R. J. (2006) Appel-Lee synthesis of glycosyl inositols, substrates for inositol dehydrogenase from Bacillus subtilis. *Carbohydr. Res. 341*, 2145−2150.

(8) Banta, S., Swanson, B. A., Wu, S., Jarnagin, A., and Anderson, S. (2002) Alteration of the specificity of the cofactor-binding pocket of Corynebacterium 2,5-diketo-D-gluconic acid reductase A. *Protein Eng. 15*, 131−140.

(9) Andreadeli, A., Platis, D., Tishkov, V., Popov, V., and Labrou, N. E. (2008) Structure-guided alteration of coenzyme specificity of formate dehydrogenase by saturation mutagenesis to enable efficient utilization of NADP(+). *FEBS J. 275*, 3859−3869.

(10) Woodyer, R., van der Donk, W. A., and Zhao, H. M. (2003) Relaxing the nicotinamide cofactor specificity of phosphite dehydrogenase by rational design. *Biochemistry 42*, 11604−11614.

(11) Didierjean, C., RahuelClermont, S., Vitoux, B., Dideberg, O., Branlant, G., and Aubry, A. (1997)) A crystallographic comparison between mutated glyceraldehyde-3-phosphate dehydrogenases from Bacillus stearothermophilus complexed with either NAD(+) or NADP(+). *J. Mol. Biol. 268*, 739−759.

(12) Petschacher, B., Leitgeb, S., Kavanagh, K. L., Wilson, D. K., and Nidetzky, B. (2005) The coenzyme specificity of Candida tenuis xylose reductase (AKR2B5) explored by site-directed mutagenesis and X-ray crystallography. *Biochem. J. 385*, 75−83.

(13) Wiegert, T., Sahm, H., and Sprenger, G. A. (1997) The substitution of a single amino acid residue (Ser-116 → Asp) alters NADP-containing glucose-fructose oxidoreductase of Zymomonas mobilis into a glucose dehydrogenase with dual coenzyme specificity. *J. Biol. Chem. 272*, 13126−13133.

(14) Dambe, T. R., Kuhn, A. M., Brossette, T., Giffhorn, F., and Scheidig, A. J. (2006) Crystal structure of NADP(H)-dependent 1,5-anhydro-D-fructose reductase from Sinorhizobium morelense at 2.2 angstrom resolution: Construction of a NADH-accepting mutant and its application in rare sugar synthesis. *Biochemistry 45*, 10030−10042.

(15) Cho, H., Oliveira, M. A., and Tai, H. H. (2003) Critical residues for the coenzyme specificity of NAD(+)-dependent 15-hydroxyprostaglandin dehydrogenase. *Arch. Biochem. Biophys. 419*, 139−146.

(16) van Straaten, K. E., Zheng, H., Palmer, D. R. J., and Sanders, D. A. R. (2010) Structural investigation of myo-inositol dehydrogenase from Bacillus subtilis: implications for catalytic mechanism and inositol dehydrogenase subfamily classification. *Biochem. J. 432*, 237−247.

(17) Carugo, O., and Argos, P. (1997) NADP-dependent enzymes 0.2. Evolution of the mono- and dinucleotide binding domains. *Proteins: Struct., Funct., Genet. 28*, 29−40.

(18) Carugo, O., and Argos, P. (1997) NADP-dependent enzymes 1. Conserved stereochemistry of cofactor binding. *Proteins: Struct., Funct., Genet. 28*, 10−28.

(19) Cornish-Bowden, A. (1995) *Analysis of Enzyme Kinetic Data*, Oxford University Press, New York.
(20) Van Straaten, K. E., Hoffort, A., Palmer, D. R. J., and Sanders, D. A. R. (2008) Purification, crystallization and preliminary X-ray analysis of inositol dehydrogenase (IDH) from Bacillus subtilis. *Acta Crystallogr., Sect. F: Struct. Biol. Cryst. Commun. 64*, 98−101.
(21) Leslie, A. W., and Powell, H. (2007) in *Evolving Methods for Macromolecular Crystallography* (Read, R., and Sussman, J., Eds.), pp 41−51, Springer: Dordrecht, The Netherlands.
(22) Evans, P. (2006) Scaling and assessment of data quality. *Acta Crystallogr., Sect. D: Biol. Crystallogr. 62*, 72−82.
(23) Rossmann, M. G., and Blow, D. M. (1962) Detection of Sub-Units within Crystallographic Asymmetric Unit. *Acta Crystallogr. 15*, 24−31.
(24) Vagin, A., and Teplyakov, A. (2010) Molecular replacement with MOLREP. *Acta Crystallogr., Sect. D: Biol. Crystallogr. 66*, 22−25.
(25) Vagin, A., and Teplyakov, A. (1997) MOLREP: an automated program for molecular replacement. *J. Appl. Crystallogr. 30*, 1022−1025.
(26) Matthews, B. W. (1968) Solvent content of protein crystals. *J. Mol. Biol. 33*, 491−497.
(27) Adams, P. D., Afonine, P. V., Bunkoczi, G., Chen, V. B., Davis, I. W., Echols, N., Headd, J. J., Hung, L.-W., Kapral, G. J., Grosse-Kunstleve, R. W., McCoy, A. J., Moriarty, N. W., Oeffner, R., Read, R. J., Richardson, D. C., Richardson, J. S., Terwilliger, T. C., and Zwart, P. H. (2010) PHENIX: a comprehensive Python-based system for macromolecular structure solution. *Acta Crystallogr., Sect. D: Biol. Crystallogr. 66*, 213−221.
(28) Emsley, P., and Cowtan, K. (2004) Coot: model-building tools for molecular graphics. *Acta Crystallogr., Sect. D: Biol. Crystallogr. 60*, 2126−2132.
(29) Moriarty, N. W., Grosse-Kunstleve, R. W., and Adams, P. D. (2009) Electronic Ligand Builder and Optimization Workbench (eLBOW): a tool for ligand coordinate and restraint generation. *Acta Crystallogr., Sect. D: Biol. Crystallogr. 65*, 1074−1080.
(30) Chen, V. B., Arendall, W. B., III, Headd, J. J., Keedy, D. A., Immormino, R. M., Kapral, G. J., Murray, L. W., Richardson, J. S., and Richardson, D. C. (2010) MolProbity: all-atom structure validation for macromolecular crystallography. *Acta Crystallogr., Sect. D: Biol. Crystallogr. 66*, 12−21.
(31) Poornam, G. P., Matsumoto, A., Ishida, H., and Hayward, S. (2009) A method for the analysis of domain movements in large biomolecular complexes. *Proteins: Struct., Funct., Bioinf. 76*, 201−212.
(32) Qi, G. Y., and Hayward, S. (2009) Database of ligand-induced domain movements in enzymes. *BMC Struct. Biol. 9*, No. 10.1186/1472-6807-9-13.
(33) Leitgeb, S., Petschacher, B., Wilson, D. K., and Nidetzky, B. (2005) Fine tuning of coenzyme specificity in family 2 aldo-keto reductases revealed by crystal structures of the Lys-274 -> Arg mutant of Candida tenuis xylose reductase (AKR2B5) bound to NAD(+) and NADP(+). *FEBS Lett. 579*, 763−767.
(34) Naylor, C. E., Gover, S., Basak, A. K., Cosgrove, M. S., Levy, H. R., and Adams, M. J. (2001) NADP(+) and NAD(+) binding to the dual coenzyme specific enzyme Leuconostoc mesenteroides glucose 6-phosphate dehydrogenase: different interdomain hinge angles are seen in different binary and ternary complexes. *Acta Crystallogr., Sect. D: Biol. Crystallogr. 57*, 635−648.
(35) Richter, N., Zienert, A., and Hummel, W. (2011) A single-point mutation enables lactate dehydrogenase from Bacillus subtilis to utilize NAD(+) and NADP(+) as cofactor. *Eng. Life Sci. 11*, 26−36.